Fractional Order PID Design for Nonlinear Motion Control Based on Adept 550 Robot

Yuquan Wan
Purdue University
yawn@purdue.edu

Haiyan Zhang
Purdue University
hhzhang@purdue.edu

Richard Mark French
Purdue University
rmfrench@purdue.edu

Abstract

Multilink robot systems are typical nonlinear systems which generously involve in uncertain disturbances, high-dimensional system matrix and non-unique characteristic functions. The authors present the method of applying fractional order PID controller to such a nonlinear system and show the advantages of this fractional controller. In the paper, the dynamic model of the system serves as the foundation to derive the control law and objective function for the optimization design of the subjected fractional order control system. The frequency domain closed loop transaction function of the studied fractional system has been developed and the paper proceeds by the study of controllability, observability and robustly satiability. The paper demonstrated the algorithms to design and optimize the fractional order PID to the nonlinear motion control system. By conducting series numerical computation, this paper shows that the fractional order PID controller could enlarge the stable region of the multilink robot system and therefore brings superior control performance in terms of trajectory tracking. The results and procedures introduced in this paper could be practically generalized to other similar systems.

Introduction

Multilink robots are widely used in manufacturing industry, and the motion control issues of these robot systems have became popular research topics for decades since the first appear of the industry robots. Generally speaking, multilink robot systems are typical nonlinear systems and always involve in uncertain disturbances, high-dimensional system matrix and non-unique characteristic functions. The fine control of industry robots usually requires complex control systems, careful calibrations and optimizations. In industry practice, 90% of these multilink robots are controlled by PID controllers which have the merits including effectiveness, simplicity, and feasibility. Although the ordinary PID controllers can achieve

satisfactory results in most common manufacturing missions, it still lacks enough precisions in the field requires precise instruments.

The structure of ordinary PID controller is fairly straightforward. Its proportional, integral and derivative control parts can provide restoring, corrective, and counteractive force respectively. Furthermore, the corrective force introduced by integral control can overcome the steady-state error brought by proportional part and the counteractive force led by derivative control could eliminate the overshoot problem caused by the integrator. Therefore in common situation the ordinary PID controllers can always effectively achieve the control objections without obvious drawbacks. However, in modem industry, the demand for the precise control is driving people to search for improvement to the ordinary PID controllers. Fractional order PID (FoPID) introduced in this paper is a natural extension to the ordinary PID controllers based on the fractional calculus theory. Since in fractional calculus the orders of integral and derivative are not limited to integer orders anymore, people can design a new type of PID controller by replacing the ordinary order integrators and differentiators by fractional order ones. The main advantages of the FoPID controllers will include enlarged stable region, relatively feasible structure, and raised control precision.

As mentioned above, fractional calculus takes the order of integrals and derivatives as any real number. It has a history nearly as long as the ordinary calculus, which considers only integer orders [1]. Recently, the applications of this technology have been successfully found in many fields, such as viscoelasticity [2], [3] , control theory [4], [5] and electro-analytical chemistry [6,] [7]. In control theory, the general conclusion about fractional control system is that it could enlarge the stable region [8] and yield a performance at least as good as its integer counterpart. And another important advantage is that fractional integrals or derivatives are hereditary functional while the ordinary ones are point functional. It is known that the hereditary functional have the long memory characteristic [9], which means at any time it would process a total memory of past states. This unique characteristic serves as one of the important reasons for the better performance. For FoPID controllers, there are also many scholars have made tremendous contribution in the past years [10], especially in the tuning rules [11], [12], approximation [13] and stability conditions [14]. All these research works generally forms the solid foundations for the work done in this study.

In this paper, the authors apply the FoPID controllers to a nonlinear multilink robot system and take uncertain disturbances into consideration. Furthermore, the fractional orders of the integrators and differentiators used here are considered as design variables rather than pre-fixed parameters. The authors studied the stability conditions and optimization design method for the overall comprehensive performance of the FoPID controllers on the basis of the mathematical model of Adept 550 robot. As one of the most commonly used robots in the industrial production lines, the Adept 550 robot is a four-axis SCARA robot with three rotational joints and one translational joint. Since it features a small motion envelope while its speeds and payloads are relatively high, Adept 550 robot can be found in mechanical assembly, material handling, packaging, machine tending, screw driving, and many other operations requiring fast and precise automation. The authors' complete study of FoPID controllers on the model of Adept550 robot shows that the fractional controller could achieve

high precise control and bring feasible approaches to optimize the design of FoPID in other applications.

Dynamics Model of Adept 550 Robot

We have included the simplied structure of Adept 550 robot as in figure 1. When applying Denavit-Hartenberg (D-H) coordinates, one would notice that Adept 550 has the special case of parallel z axes, which is connected with the rigid inner and outer links. The trajectory of this robot is determined by the motion of these two links, and at the wrist the rotational joint rotates about the z axis to adjust the gripper angle, but not to change the trajectory. Since we mainly focus on the performance of trajectory tracking in this study, In order to focus on the trajectory study, without losing generality we would fairly assume the wrist's rotary angle is zero. If took the notations as labeled in figure 1, one could get the D-H parameters as showed in the table 1.

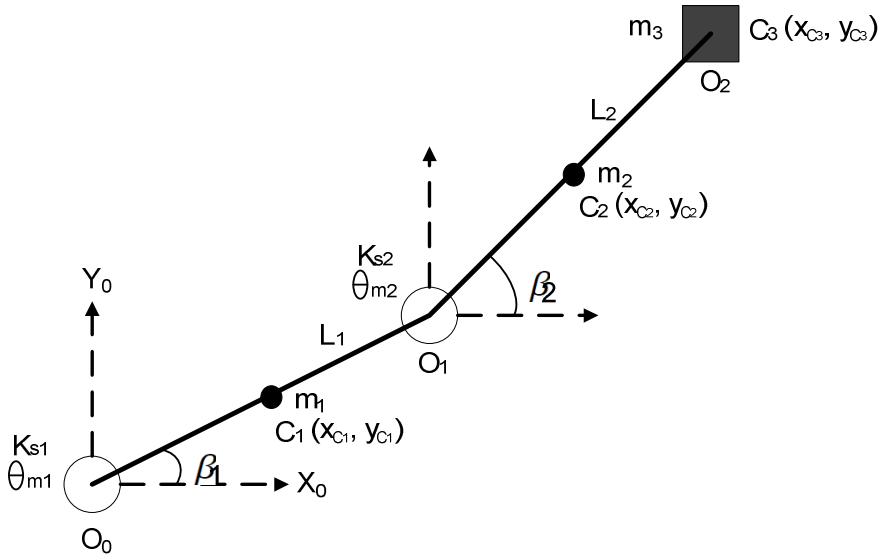

Figure 1: simplified structure of Adept 550 robot

Table 1. D-H parameters

Link	Li	i	di	i
Inner	L1	0	0	1
Outer	L2	0	0	2

Table 1 lists the D-H parameters of the inner and outer links. For the inner link (i=1) and outer link (i=2), the coordinate transformation with rotation and translation components is described with the matrix:

$$A_i = R_{z,\theta_i} T_{z,d_i} T_{x,L_i} R_{x,\alpha_i} = \begin{bmatrix} \cos\theta_i & -\sin\theta_i \cos\alpha_i & \sin\theta_i \sin\alpha_i & L_i \cos\theta_i \\ \sin\theta_i & \cos\theta_i \cos\alpha_i & -\cos\theta_i \sin\alpha_i & L_i \sin\theta_i \\ 0 & \sin\alpha_i & \cos\alpha_i & d_i \\ 0 & 0 & 0 & 1 \end{bmatrix} \quad (1)$$

The simplified transformation matrix of Adept 550 from the base to the gripper is as follows:

$$T_0^2 = A_1 A_2 = \begin{bmatrix} \cos(\theta_1+\theta_2) & -\sin(\theta_1+\theta_2) & 0 & L_1\cos\theta_1 + L_2\cos(\theta_1+\theta_2) \\ \sin(\theta_1+\theta_2) & \cos(\theta_1+\theta_2) & 0 & L_1\sin\theta_1 + L_2\sin(\theta_1+\theta_2) \\ 0 & 0 & 1 & 0 \\ 0 & 0 & 0 & 1 \end{bmatrix} \quad (2)$$

Noticing the relationships the angular position β_i $(i = 1,2)$ of the motors and the angle θ_i $(i = 1,2)$ about previous z from old x to new x: $\beta_1 = \theta_1$, $\beta_2 = \theta_1 + \theta_2$, the gripper's horizontal position (P_x, P_y) can be expressed as

$$\begin{aligned} P_x &= L_1 \cos\beta_1 + L_2 \cos\beta_2 \\ P_y &= L_1 \sin\beta_1 + L_2 \sin\beta_2 \end{aligned} \quad (3)$$

From Equation (3), the motor angular positions (β_1, β_2) can be derived:

$$\begin{aligned} \beta_1 &= 2\tan^{-1}\left(\frac{P_y \pm \sqrt{P_x^2 + P_y^2 - R_1}}{P_x + R_1}\right) \\ \beta_2 &= 2\tan^{-1}\left(\frac{P_y \pm \sqrt{P_x^2 + P_y^2 - R_2}}{P_x + R_2}\right) \end{aligned} \quad (4)$$

Where:

$$\begin{aligned} R_1 &= \frac{P_x^2 + P_y^2 + L_1^2 - L_2^2}{2L_1} \\ R_2 &= \frac{P_x^2 + P_y^2 + L_2^2 - L_1^2}{2L_2} \end{aligned} \quad (5)$$

The forward velocity v can be found from Equation (3):

$$v = \begin{pmatrix} \dot{P}_x \\ \dot{P}_y \end{pmatrix} = J_a \begin{pmatrix} \dot{\beta}_1 \\ \dot{\beta}_2 \end{pmatrix} \quad (6)$$

Where J_a is Jacobian matrix

$$J_a = \begin{bmatrix} -L_1 \sin\beta_1 & -L_2 \sin\beta_2 \\ L_1 \cos\beta_1 & L_2 \cos\beta_2 \end{bmatrix} \tag{7}$$

And the backward velocity $(\dot{\beta}_1, \dot{\beta}_2)$ can be derived as follows:

$$\begin{pmatrix} \dot{\beta}_1 \\ \dot{\beta}_2 \end{pmatrix} = J^{-1} \begin{pmatrix} \dot{P}_x \\ \dot{P}_y \end{pmatrix} \tag{8}$$

Also, the relationships of the forward acceleration $(\ddot{P}_x, \ddot{P}_y)$ can be determined:

$$\begin{pmatrix} \ddot{P}_x \\ \ddot{P}_y \end{pmatrix} = J_a \begin{pmatrix} \ddot{\beta}_1 \\ \ddot{\beta}_2 \end{pmatrix} + J_v \begin{pmatrix} \dot{\beta}_1^2 \\ \dot{\beta}_2^2 \end{pmatrix} \tag{9}$$

Where:

$$J_v = \begin{bmatrix} -L_1 \cos\beta_1 & -L_2 \cos\beta_2 \\ -L_1 \sin\beta_1 & -L_2 \sin\beta_2 \end{bmatrix} \tag{10}$$

The relationships of the backward acceleration $(\ddot{\beta}_1, \ddot{\beta}_2)$ are as follows:

$$\begin{pmatrix} \ddot{\beta}_1 \\ \ddot{\beta}_2 \end{pmatrix} = J_a^{-1} \begin{pmatrix} \ddot{P}_x \\ \ddot{P}_y \end{pmatrix} - J_a^{-1} J_v \begin{pmatrix} \dot{\beta}_1^2 \\ \dot{\beta}_2^2 \end{pmatrix} \tag{11}$$

Applying the Lagrange method, one could get the dynamics of Adept 550 robot as described below [15]:

$$D(\beta)\ddot{\beta} + H(\beta, \dot{\beta})\dot{\beta} + G(\beta) = \tau + \tau_{damping} \tag{12}$$

Where:

$$D(\beta) = \begin{bmatrix} \left(\frac{7}{12}m_1 + m_2 + m_3\right)L_1^2 & \left(\frac{1}{2}m_2 + m_3\right)L_1 L_2 \cos(\beta_2 - \beta_1) \\ \left(\frac{1}{2}m_2 + m_3\right)L_1 L_2 \cos(\beta_2 - \beta_1) & \left(\frac{7}{12}m_2 + m_3\right)L_2^2 \end{bmatrix} \tag{13.a}$$

$$H(\beta,\dot{\beta})=\begin{bmatrix} 0 & -\left(\frac{1}{2}m_2+m_3\right)L_1L_2\sin(\beta_2-\beta_1)\dot{\beta}_2 \\ \left(\frac{1}{2}m_2+m_3\right)L_1L_2\sin(\beta_2-\beta_1)\dot{\beta}_1 & 0 \end{bmatrix} \tag{13.b}$$

$$G(\beta)=\begin{pmatrix} \left(\frac{1}{2}m_1+m_2+m_3\right)gL_1\cos\beta_1-k_{s1}\left(r\theta_{m1}-\beta_1\right) \\ \left(\frac{1}{2}m_2+m_3\right)gL_2\cos\beta_2-k_{s2}\left(r\theta_{m2}-\beta_2\right) \end{pmatrix} \tag{13.c}$$

$$\tau=\begin{pmatrix}\tau_1\\ \tau_2\end{pmatrix} \tag{13.d}$$

$$\tau_{damping}=\begin{pmatrix}\tau_{damping1}\\ \tau_{damping2}\end{pmatrix}=\begin{bmatrix}-C_1 & 0\\ 0 & -C_2\end{bmatrix}\begin{pmatrix}\dot{\beta}_1\\ \dot{\beta}_2\end{pmatrix}=C\begin{pmatrix}\dot{\beta}_1\\ \dot{\beta}_2\end{pmatrix} \tag{13.e}$$

And matrix C is composed of the damping coefficients.

Model of fractional order PID controllers

Based on equation (12), we can assume that the motors driving the inner and outer links are in the same type. Dynamics of the two links is described as:

)$For:\quad k=1,\quad 2$

$$\sum_{j=1}^{n}d_{jk}(\beta)\ddot{\beta}_j+\sum_{i,j=1}^{n}h_{ijk}(\beta)\dot{\beta}_i\dot{\beta}_j+g_k(\beta)=\tau_k-C_k\dot{\beta}_k, \tag{14}$$

$$J_{m,k}\ddot{\theta}_{mk}+\left(B_{m,k}+K_{b,k}\frac{K_{m,k}}{R_k}\right)\dot{\theta}_{mk}=\frac{K_{m,k}}{R_k}V_k-\tau_{m,k}$$

Since $\beta_k=r\theta_{m,k}$, $\tau_{m,k}=r\tau_k$, where r is the gear ratio, the two dynamic equations of robot link and its driving motor expressed in Equation (14) can be combined into a single one:

$$J_{eff,k}\ddot{\theta}_{mk}+B_{eff,k}\dot{\theta}_{mk}=KV_k-C_k\theta_{mk}-rd_k,\qquad k=1,2 \tag{15}$$

Now for a fractional order PID controller, $PI^{\lambda}D^{\mu}$, one has the five design parameters as summarized in table 2:

Table 2. design parameters for the controller

K_P	Coefficient for the proportional term
K_D	Coefficient for the derivative term
K_I	Coefficient for the integral term
μ	Fractional order for the derivative term
λ	Fractional order for the integral term

The close loop control diagram is showed in figure 2, and equation (16) describes the transfer function of this close loop system . The fractional derivative used in this study is defeined ad Caputo's fractional derivative [16].

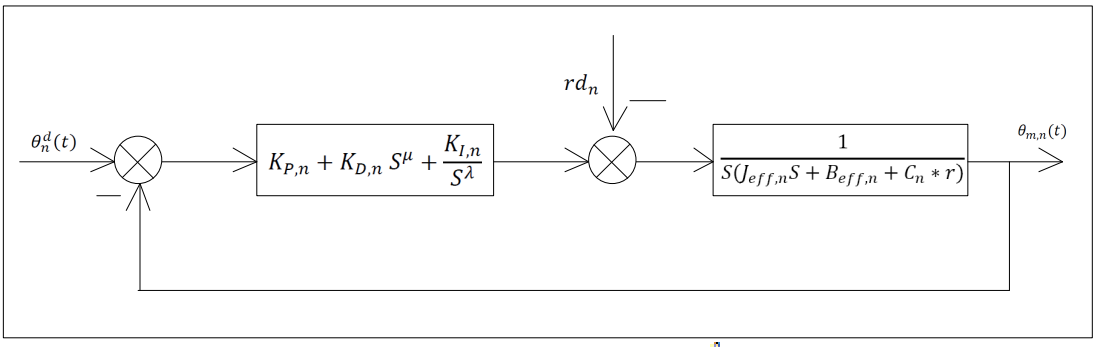

Figure 2, close loop diagram of fractional order $PI^{\lambda}D^{\mu}$ controlled robot arm

$$\theta_{m,n} = \frac{(K_P\theta_n^d - rd_n)S^{\lambda} + K_{I,n}\theta_n^d}{J_{eff,n}S^{\lambda+2} + (B_{eff,n} + C_n r)S^{\lambda+1} + K_{p,n}S^{\lambda} + K_{I,n}} \tag{16}$$

In this research we consider the FoPID controllers in the two arms have the same fractional order λ and μ but different coefficients. Besides, both the fractional order of the integrator and the differentiator are bounded in the range of (0, 1) in this study.

In equation (16), the non-linear terms d_n is as equation (17)

$$\begin{aligned} d_1 &= (\tfrac{1}{2}m_2 + m_3)\{L_1L_2\cos(\beta_2 - \beta_1)\ddot{\beta}_2 - L_1L_2\sin(\beta_2 - \beta_1)\dot{\beta}_2^2\} + (\tfrac{1}{2}m_1 + m_2 + m_3)gL_1\cos\beta_1 \\ d_2 &= (\tfrac{1}{2}m_2 + m_3)\{L_1L_2\cos(\beta_2 - \beta_1)\ddot{\beta}_1 - L_1L_2\sin(\beta_2 - \beta_1)\dot{\beta}_1^2 + gL_2\cos\beta_2 \end{aligned} \tag{17}$$

Apply the Caputo's fractional order derivative to (17), and since $\beta_K = r\theta_{m,K}$, we could have the time domain system function in matrix representation as in (18).

$$\begin{bmatrix} J_{eff,1} & r^2T_1 \\ r^2T_1 & J_{eff,2} \end{bmatrix}\begin{bmatrix} {}_0D_t^{\lambda+2}\beta_1 \\ {}_0D_t^{\lambda+2}\beta_2 \end{bmatrix}+\begin{bmatrix} B_{eff,1}+c_1r & r^2T_2\dot{\beta}_2^{\,2-\lambda} \\ r^2T_2\dot{\beta}_1^{\,2-\lambda} & B_{eff,2}+c_2r \end{bmatrix}\begin{bmatrix} {}_0D_t^{\lambda+2}\beta_1 \\ {}_0D_t^{\lambda+2}\beta_2 \end{bmatrix}+$$
$$+\begin{bmatrix} K_{P1}+r^2(-T_3\ddot{\beta}_2+T_4\dot{\beta}_2^{\,2}+T_5) & r^2(T_3\ddot{\beta}_2-T_4\dot{\beta}_2^{\,2}) \\ r^2(-T_3\ddot{\beta}_1+T_4\dot{\beta}_1^{\,2}) & K_{P2}+r^2(T_3\ddot{\beta}_1-T_4\dot{\beta}_1^{\,2}+T_6) \end{bmatrix}\begin{bmatrix} {}_0D_t^{\lambda}\beta_1 \\ {}_0D_t^{\lambda}\beta_2 \end{bmatrix} \qquad (18)$$
$$+\begin{bmatrix} K_{D1} & 0 \\ 0 & K_{D2} \end{bmatrix}\begin{bmatrix} {}_0D_t^{\lambda+\mu}\beta_1 \\ {}_0D_t^{\lambda+\mu}\beta_2 \end{bmatrix}+\begin{bmatrix} K_{I1} & 0 \\ 0 & K_{I2} \end{bmatrix}\begin{bmatrix} \beta_1 \\ \beta_2 \end{bmatrix}=$$
$$=\begin{bmatrix} K_{P1} & 0 \\ 0 & K_{P2} \end{bmatrix}\begin{bmatrix} {}_0D_t^{\lambda}\beta_1^{\,d} \\ {}_0D_t^{\lambda}\beta_2^{\,d} \end{bmatrix}+\begin{bmatrix} K_{D1} & 0 \\ 0 & K_{D2} \end{bmatrix}\begin{bmatrix} {}_0D_t^{\lambda+\mu}\beta_1^{\,d} \\ {}_0D_t^{\lambda+\mu}\beta_2^{\,d} \end{bmatrix}+\begin{bmatrix} K_{I1} & 0 \\ 0 & K_{I2} \end{bmatrix}\begin{bmatrix} {}_0D_t^{\lambda}\beta_1^{\,d} \\ {}_0D_t^{\lambda}\beta_2^{\,d} \end{bmatrix}$$

Where in (18):

$$T_1=\left(\frac{1}{2}m_2+m_3\right)L_1L_2\cos(\beta_2-\beta_1) \qquad (19.a)$$

$$T_2=-\left(\frac{1}{2}m_2+m_3\right)L_1L_2\sin(\beta_2-\beta_1)\frac{\Gamma(3)}{\Gamma(3-\lambda)} \qquad (19.b)$$

$$T_3=\left(\frac{1}{2}m_2+m_3\right)L_1L_2\cos(\beta_2-\beta_1+\lambda\frac{\pi}{2}) \qquad (19.c)$$

$$T_4=\left(\frac{1}{2}m_2+m_3\right)L_1L_2\sin(\beta_2-\beta_1+\lambda\frac{\pi}{2}) \qquad (19.d)$$

$$T_5=\left(\frac{1}{2}m_1+m_2+m_3\right)gL_1\cos(\beta_1+\lambda\frac{\pi}{2}) \qquad (19.e)$$

$$T_6=\left(\frac{1}{2}m_2+m_3\right)gL_2\cos(\beta_2+\lambda\frac{\pi}{2}) \qquad (19.f)$$

In equation (18), the differential order of the β_1 β_2 are $\lambda+2$, $\lambda+1$, $\lambda+\mu$ and 0. Since these orders are not equally spaced, it is not easy to directly re-write (18) in a linear matrix formation. Inspired by the work of Galkowski, Bachelier, and Kummert [17], we assume λ and μ are rational numbers which could be expressed by $\frac{a}{b}$ and $\frac{c}{d}$ in their relatively prime formats respectively. By noting $\beta=[\beta_1;\beta_2]$ equation (18) could be written as in (20):

$$M_1\,{}_0D_t^{\frac{ac+2bd}{bd}}\beta+M_2\,{}_0D_t^{\frac{ac+bd}{bd}}\beta+M_3\,{}_0D_t^{\frac{ac+bc}{bd}}\beta+M_4\,{}_0D_t^{\frac{ad}{bd}}\beta+M_5\,{}_0D_t^{\frac{0}{b}}\beta-U=0 \qquad (20)$$

In (20), M_i and U are coefficient matrix containing their corresponding terms in (18). One more thing to mention here is not all of these coefficients are constant since the uncertain disturbance. We will show (20) is actually a time variant system later. By inserting zero matrixes, it is equivalent to write (20) as in (21):

$$
\begin{aligned}
&M_{10}D_t^{\frac{ac+2bd}{bd}}\beta+N_{10}D_t^{\frac{ac+2bd-1}{bd}}\beta+N_{20}D_t^{\frac{ac+2bd-2}{bd}}\beta+\cdots+M_{20}D_t^{\frac{ac+bd}{bd}}\beta+\\
&+N_{i0}D_t^{\frac{ac+bd-1}{bd}}\beta+\cdots+M_{30}D_t^{\frac{ac+bc}{bd}}\beta+\cdots+N_{j0}D_t^{\frac{ad+1}{bd}}\beta+\\
&+M_{40}D_t^{\frac{ad}{bd}}\beta+\cdots+N_{k0}D_t^{\frac{a+1}{bd}}\beta+M_{50}D_t^{\frac{0}{b}}\beta-U=0
\end{aligned}
\tag{21}
$$

Where $N_1=N_2=\cdots=N_i=\cdots=N_j=N_K=0$ .Based on (21) one has an equally spaced fractional order system on every term, and therefore the state space could be defined as:

$$
x=\begin{bmatrix} {}_0D_t^{\frac{0}{bd}}\beta & {}_0D_t^{\frac{1}{bd}}\beta & \cdots & {}_0D_t^{\frac{ad-1}{bd}}\beta & {}_0D_t^{\frac{ad}{bd}}\beta & \cdots & {}_0D_t^{\frac{ad+2bd-1}{bd}}\beta \end{bmatrix}^T \tag{22}
$$

And the system is:

$$
{}_0D_t^{\frac{1}{bd}}X=AX+BU \tag{23}
$$

Where:

$$
A=\begin{bmatrix} 0_{[2ad+4bd-2,2]} & \vdots & I_{[2ad+4bd-2,2ad+4bd-2]} \\ \cdots & \cdots & \cdots \\ -M_1^{-1}M_5 \quad 0\cdots & -M_1^{-1}M_4 \quad 0\cdots & -M_1^{-1}M_3 \quad 0\cdots \quad -M_1^{-1}M_2 \quad 0\cdots \end{bmatrix} \tag{24.a}
$$

$$
B=\begin{bmatrix} 0_{[2ad+4bd-2,2]} & \\ \cdots & \cdots \\ 1 & 0 \\ 0 & 2 \end{bmatrix} \tag{24.b}
$$

In (24.a) and (24.b), $0_{[2ad+4bd-2,2]}$ is a zero matrix whose dimension is $[2ad+4bd-2,2]$ and $I_{[2ad+4bd-2,2ad+4bd-2]}$ is the identity matrix has the dimension of $[2ad+4bd-2,2ad+4bd-2]$. Equation (23) is the state space reprenstation of our system function. The system matrix A has the dimesion of $[2ad+4bd,2ad+4bd]$ and B has the dimention of $[2ad+4bd,2]$. The stability study and the design of the fractional order PID controller will focus on the matrix A. Although, A could have a very high dimension with the different fractional order, the fact that matrix A is a sparse matrix makes the task easier in most cases.

Controllable, observable, and robust stable of the system:

Since matrix *A* is in the controllable canonical form and consequently one state could be transferred to another, the system is controllable and observable. The design focuses on the robust stable of this system. For a fractional order system, the system would be guaranteed stable if all the system matrix's eigenvalues satisfy the following criteria [18].

$$\left|\arg(\lambda)\right| > \beta\frac{\pi}{2} \tag{25}$$

Therefore, in this study the ratio of stable region of FoPID to the integer PID is $2-1/bd$ One seems could rising *b* and *d* to get a larger stable region. However, rising them will cause a larger dimension of matrix *A* and involves more eigenvalues, since the total number of eigenvalues is *2ad+4bd*. More eigenvalues would make it harder to grantee all of them are settled in the stable region.

Moreover, since *A* is a bounded sparse matrix with interval uncertainties, there should be infinite numbers of eigenvalues to check to satisfy the stable region if one directly use the method in (25). In this case, we would like to check the boundaries of each eigenvalue [18], [19], and continue to analysis the stabilities of the system based on the behaviors of all eigenvalues' boundaries [20]. Therefore we need to check the boundaries of this system matrix *A*. Based on (18) and (19), the following inequality holds:

$$J_{eff,1}J_{eff,2} > r^2 J_m[L_1^2(\frac{1}{2}m_1 + m_2 + m_3) + L_2^2(\frac{1}{2}m_2 + m_3)] + r^4(\frac{1}{2}m_2 + m_3)^2 L_1^2 L_2^2 \tag{26}$$

Thus, the determinant of matrix M_1 satisfies:

$$J_{eff,1}J_{eff,2} - r^4 T_1^2 \neq 0 \tag{27}$$

The fact that condition (27) always holds implies the matrix M_1 is always nonsingular and consequently the matrix *A* will never be singular if $K_{i1} \neq 0, K_{i2} \neq 0$. And in this design we will keep this condition. Thus, we have:

$$\frac{1}{\det(M_1)} \in [\frac{1}{J_{eff,1}J_{eff,2}}, \frac{1}{J_{eff,1}J_{eff,2} - r^4(0.5m_2 + m_3)^2 L_1^2 L_2^2}] \tag{28}$$

And in this robot control study the $\dot{\beta}$ and $\ddot{\beta}$ are also bounded because of reality. Therefore one could find the matrix *A* is bounded. Plug in the parameters we used in this study, we get the following boundary functions for each variant terms in *A* through numerical computation, the boundaries are functions of design parameters $(K_{I1}, K_{I2}, K_{P1}, K_{P2}, K_{D1}, K_{D2}, \lambda, \mu)$.

$$\begin{aligned} \overline{-M_1^{-1}M_5} &= \begin{bmatrix} -57.2273K_{I1} & 94.6367K_{I2} \\ 94.6367K_{I1} & -229.4504K_{I2} \end{bmatrix} \\ \underline{-M_1^{-1}M_5} &= \begin{bmatrix} -83.7362K_{I1} & -64.9431K_{I2} \\ -64.9431K_{I1} & -335.73674K_{I2} \end{bmatrix} \end{aligned} \tag{29.a}$$

$$\overline{-M_1^{-1}M_4} = \begin{bmatrix} 48.1076 - 71.7260K_{P1} & 27.5032 + 93.6562K_{P2} \\ 87.6325 + 71.3310K_{P1} & 98.6555 - 262.3100K_{P2} \end{bmatrix}$$
$$\underline{-M_1^{-1}M_4} = \begin{bmatrix} -44.5903 - 80.7186K_{P1} & -31.5653 - 64.9431K_{P2} \\ -96.3535 - 46.8943K_{P1} & -91.9135 - 308.9341K_{P2} \end{bmatrix} \quad (29.b)$$

$$\overline{-M_1^{-1}M_3} = \begin{bmatrix} -57.2273K_{D1} & 94.6367K_{D2} \\ 94.6367K_{D1} & -229.4504K_{D2} \end{bmatrix}$$
$$\underline{-M_1^{-1}M_3} = \begin{bmatrix} -83.7362K_{D1} & -64.9431K_{D2} \\ -64.9431K_{D1} & -335.73674K_{D2} \end{bmatrix} \quad (29.c)$$

$$\overline{-M_1^{-1}M_2} = \begin{bmatrix} -5.7227 + 0.0711\dot{\beta}_{1,MAX}^{2-\lambda} & 9.4637 \\ 9.4637 + 0.2069\dot{\beta}_{1,MAX}^{2-\lambda} & -22.945 + 0.0609\dot{\beta}_{2,MAX}^{2-\lambda} \end{bmatrix}$$
$$\underline{-M_1^{-1}M_2} = \begin{bmatrix} -8.3736 & -6.4943 - 0.4241\dot{\beta}_{2,MAX}^{2-\lambda} \\ -6.4943 - 1.7004\dot{\beta}_{1,MAX}^{2-\lambda} & -33.5737 \end{bmatrix} \quad (29.d)$$

Now, we could study the robust stability of this FoPID controlled system at different design $(K_{I1}, K_{I2}, K_{P1}, K_{P2}, K_{D1}, K_{D2}, \lambda, \mu)$. And this feature actually provides a criterion to optimize the design of the controllers. Next we would like to show how the design parameters, which are the coefficients and the fractional order of the two FoPID controllers, affect the robust stability. The figure 3 shows this effect. Taking the upper left frame in figure 3 as an example, the rectangles drew by blue solid lines show the boundaries of each eigenvalues. Since there are uncertainties involved in this system the eigenvalues are actually located in a range rather than single spots. And rectangles provide sufficient boundaries for this eigenvalues [19]. To ensure the system is robustly stable, the eigenvalues' boundaries are not allowed to cross the stable boundary, which essentially represent the angle represents the angle $\pm 2\pi / bd$ in this research. For a better demonstration, we plot those non-violated stable boundaries by cyan solid lines and those violated stable boundaries by red solid lines.

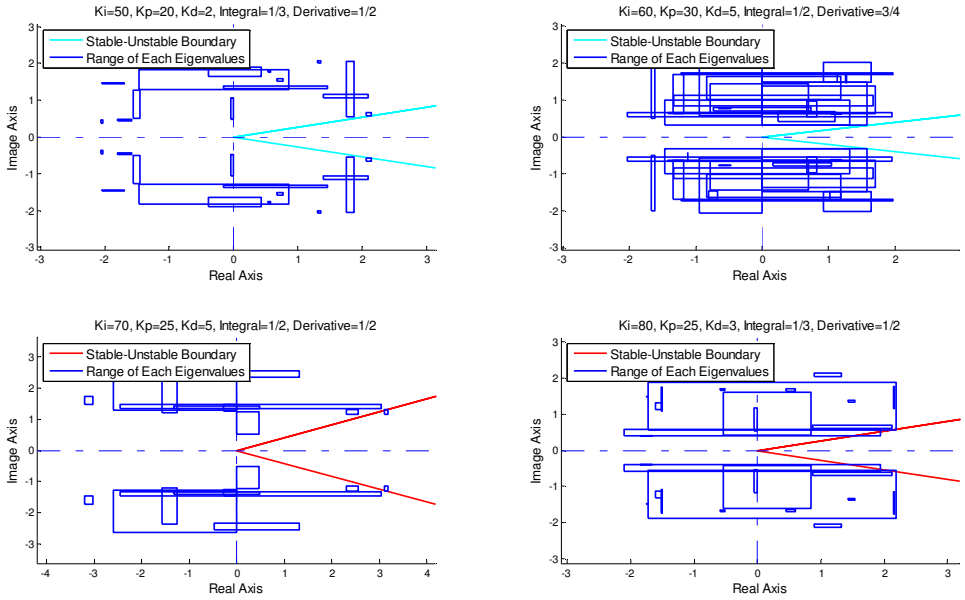

Figure 3: the effect of changing design variables to the overall stability

Figure 3 clearly shows that changing the combination of the design variables could bring changes on the overall stability to the whole system. During the design of the whole parameters set, there could be unlimited permutations for the choices of design variable set $(K_{I1}, K_{I2}, K_{P1}, K_{P2}, K_{D1}, K_{D2}, \lambda, \mu)$. The authors would like to apply some optimization algorithm to achieve the comprehensive optimized design. Since task of optimization design involves the permutation of each parameter, the genetic algorithm is a natural choice for this mission.

Optimization Design

For this design, the system contains uncertainties and one could only obtain the ranges for each eigenvalues. Like showed in figure 3, the ranges are the rectangles bounded by every four corner eigenvalues. If we draw down this corner eigenvalues in a complex plain and note the arguments of them by $\angle\beta_{ij}, i = 1,2,\ldots n; j = 1,2,3,4$ one could then measure the difference of these arguments to the stable boundary. In this way and combined with the facts that all eigenvalues are symmetrical to real axis in the complex plan, a natural optimization objective is to minimize the difference of stable arguments, $2\pi / bd$, to the absolute value of each $\angle\beta_{ij}$. Therefore, the optimization function used in this research is expressed as following equation (30):

$$OptimalDesign(K_{I1}, K_{I2}, K_{P1}, K_{P2}, K_{D1}, K_{D2}, \lambda, \mu) = \arg\min \sum_{i=1}^{n} \sum_{j=1}^{4} \psi_{ij} \left(\frac{2\pi}{bd} - \left| \angle\beta_{ij} \right| \right) \qquad (30)$$

In (30), ψ_{ij} serves as the coefficient of penalization. There could be many methods to assign the values of ψ_{ij}. And also one could separate the complex plain into different segments

according to various criteria. In this paper we studied the two-zone penalization method and three-zone penalization methods, and they are all stepwise penalization methods. And table 3 in the following summarized these two different methods.

Table 3: value of penalization coefficient

Two-Zone Method		Three-Zone Method	
$\lvert\angle\beta_{ij}\rvert$	ψ_{ij}	$\lvert\angle\beta_{ij}\rvert$	ψ_{ij}
$\in [0,2\pi/bd]$	1e+5	$\in [0,2\pi/bd]$	1e+10
$\in (2\pi/bd,\pi]$	1	$\in (2\pi/bd,0.5\pi+2\pi/bd]$	1e+3
N/A	N/A	$\in (0.5\pi+2\pi/bd,\pi]$	1

Before exploring the trajectory tracking performance, we would like to introduce the trajectory planning used in this study. We are going to let the robot arm move in both x-direction and y-direction. We set the original point at (500 mm, 320 mm) and allow 1 second for the robot arm to move to position (200 mm, 600mm). Figure 4 demonstrates the trajectory plan. We also summarized the optimization results in the table 4.

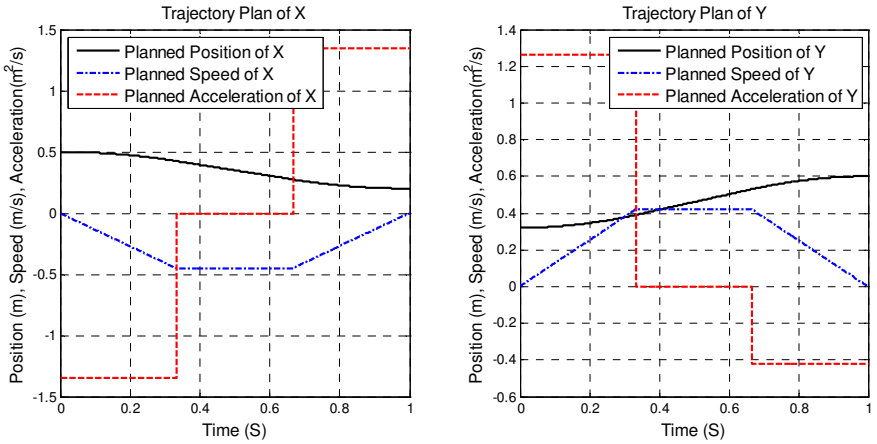

Figure 4: trjectory plan

Table 4. optimization results of design parameters

Two-Zone Method		Three-Zone Method	
K_{P1}	146.93	K_{P1}	93.87
K_{P2}	14.27	K_{P2}	80.60
K_{I1}	67.33	K_{I1}	14.27
K_{I2}	80.60	K_{I2}	146.93
K_{D1}	0.80	K_{D1}	4.70
K_{D2}	3.50	K_{D2}	0.80
λ	0.20	λ	0.67
μ	0.83	μ	0.75

Simulation results and conclusions

We have plotted the simulation results about the trajectory tracking in the figure 5. This figure includes the results from the system optimized by both the two-zone method and three-zone method. And to compare with, we have also included an ordinary PID controller result [15]. As showed in figure 5, the optimized FoPID controllers have tracked the trajectory plan successfully. In terms of tracking error, the fractional system achieved a higher precision when comparing with the ordinary PID system. Both of the two-zone method and three-zone method provide satisfactory optimization results and therefore the optimization method studied in this paper has been justified as effective one. We also recorded the tracking error at each sampling point, and computed the average squared tracking error as summarized in table 5. From table 5, one could clearly see that the FoPID systems have raised the precision of tracking by one order of magnitude.

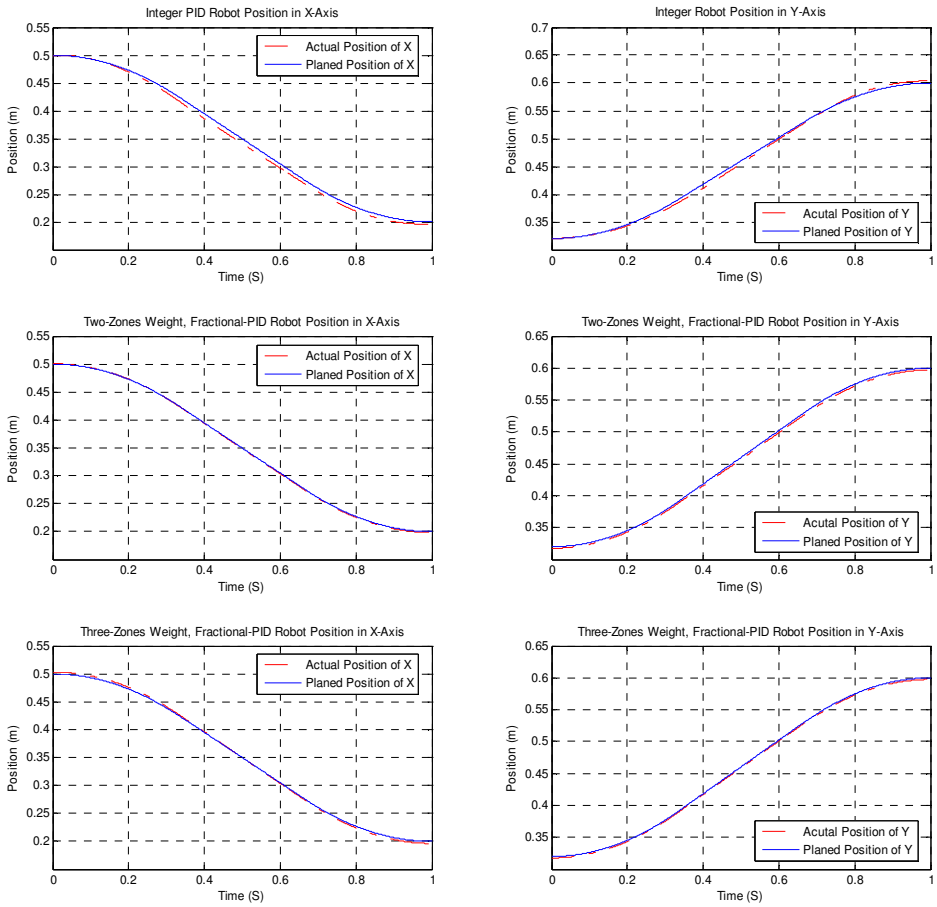

Figure 10: Simulation comparisons, in terms of trajectory tracking

Table 6. comparisons in terms of mean squared tracking errors

	Ordinary PID	FoPID, Two-Zones	FoPID, Three-Zones
Mean Squared Error in X	3.8859e-05	1.2279e-6	7.0355e-6
Mean Squared Error in Y	1.4879e-05	8.8149e-6	3.7683e-6

Evidenced by the simulation results, the FoPID controlled Adept550 robot system could achieve a better result in terms of trajectory tracking. And the design methods introduced in this paper is effective when finding the optimized design of the fractional controllers. This method could be easily transferred into other applications related to fractional control, and consequently bring valuable results to industry practice. In the end, we would like to conclude the following points:

1. The fractional order control of multilink robot system always involves disturbance or other uncertainties, therefore studying the limits of each eigenvalues is a feasible method to analysis the overall stability. Furthermore, the boundary matrix could be helpful in finding the optimization design of the fractional order controllers.

2. The stepwise penalized method could be used to optimize the design of FoPID system, and this method allows people to move the system eigenvalues toward to the desired regions. The method proposed in this paper could be generalized to other application in the design of fractional order controllers.

3. The optimized fractional system will take the advantage of the enlarged stable region while avoiding any negative effects brought by the increased number of eigenvalues. Simulation results show that the optimized FoPID controlled Adept550 system could track the planned trajectory successfully and raise the precision greatly during the tracking process. This characteristic would bring valuable result to the manufacturing industry.

References

[1] Loverro A., Fractional Calculus: History, Definitions and Applications for the Engineer, 2004

[2] Mainardi F., Applications of Fractional Calculus in Mechanics, Transform Methods and Special Functions, Varna'96, SCT Publishers, Singapore, 1997.

[3] Rossikhin Y.A, Shitikova M.V., Applications of Fractional Calculus to Dynamic Problems of Linear and Nonlinear Hereditary Mechanics of Solids, Appl. Mech. Rev. 50,15-67, 1997.

[4] Bagley R.L. and Calico R.A., Fractional Order State Equations for the Control of Viscoelastically Damped Structures, J.Guidance, vol. 14, no. 5 pp.304-311, 1991

[5] Makroglou A., Miller R.K. and Skkar S., Computational Results for a Feedback Control for a Rotating Viscoelastic Beam, J of Guidance, Control and Dynamics, vol. 17, no. 1, pp. 84-90, 1994.
[6] Oldham K.B., A Signal Independent Electro-analytical Method, Anal. Chem., vol.72 pp.371-378, 1976
[7] Goto M. and Ishii D., Semi-differential Electro-analysis, J. Electro anal. Chem. and Interfacial Electrochemical., vol.61, pp.361-365, 1975
[8] D. Matignon, Generalized Fractional Differential and Difference Equations: Stability Properties and Modelling Issues. Proc. of Math.Theory of Networks and Systems Symposium, Padova, Italy, 1998.
[9] Diethelm, K., N. J. Ford, et al. (2005). "Algorithms for the fractional calculus: A selection of numerical methods." Computer Methods in Applied Mechanics and Engineering 194(6-8): 743-773.
[10] I. Podlubny, Fractional-Order Systems and Fractional-Order Controllers, Inst. Exp. Phys., Slovak Acad. Sci., Vol.4, No.2, 1994, pp.28-34.
[11] Ying Luo; YangQuan Chen; , "Fractional-order [proportional derivative] controller for robust motion control: Tuning procedure and validation," American Control Conference, 2009. ACC '09. , vol., no., pp.1412-1417, 10-12 June 2009
[12] Dingyu Xue; YangQuan Chen; , "Fractional Order Calculus and Its Applications in Mechatronic System Controls Organizers," Mechatronics and Automation, Proceedings of the 2006 IEEE International Conference on , vol., no., pp.nil33-nil33, June 2006
[13] Dingyu Xue; Chunna Zhao; YangQuan Chen; , "A Modified Approximation Method of Fractional Order System," Mechatronics and Automation, Proceedings of the 2006 IEEE International Conference on , vol., no., pp.1043-1048, 25-28 June 2006
[14] Jocelyn Sabatier, Mathieu Moze, Christophe Farges, LMI stability conditions for fractional order systems, Computers & Mathematics with Applications, Volume 59, Issue 5, Fractional Differentiation and Its Applications, March 2010, Pages 1594-1609, ISSN 0898-1221
[15] Henry Zhang, PID Controller Design for A Nonlinear Motion Control Based on Modeling the Dynamics of Adept 550 Robot, International Journal of INdustrial Engineering and Management (IJIEM), Vol. 1, No.1, 2010
[16] El-Sayed A. M. A., Multivalued Fractional Differential Equations, Applied. Math and Computer, vol. 80, pp. 1-11, 1994
[17] Galkowski, K.; Bachelier, O.; Kummert, A.; , "Fractional Polynomials and nD Systems: A Continuous Case," *Decision and Control, 2006 45th IEEE Conference on* , vol., no., pp.2913-2917, 13-15 Dec. 2006
[18] A.S. Deif, The interval eigenvalue problem, Z. Angew. Math. Mech. 71 (1) (1991) 61–64.
[19] YangQuan Chen; Hyo-Sung Ahn; Podlubny, I.; , "Robust stability check of fractional order linear time invariant systems with interval uncertainties," *Mechatronics and Automation, 2005 IEEE International Conference* , vol.1, no., pp. 210- 215 Vol. 1, 29 July-1 Aug. 2005
[20] Z. Qiu, P.C. Müller, A. Frommer, An appliximation method for the standard interval eigenvalue problem of real nonsymmetric interval matrices, Comm. Numer. Methods Eng. 17 (2001) 239-251.

Biography

YUEQUAN WAN is currently a PhD candidate in Purdue Unviersity, his research focuses on applied fractional calculus and fractional order control.

HAIYAN ZHANG is an assistant professor at Purdue Univiersity, his research covers control, applied fractional calculus, hydraulics, machining, and multi-dissinpline design optimization. Dr. Zhang got his PhD from university of Michigan.

RICHARD MARK FRENCH is an associate professor at Purdue Unviersity. his research focuses on applied fractional calculus, music acousitics, aeroelastics and optimization. Dr. French got his PhD from university of Dayton.